HHS Public Access

Author manuscript

*J Neurochem*. Author manuscript; available in PMC 2018 May 01.

Published in final edited form as:

*J Neurochem*. 2017 May ; 141(3): 423–435. doi:10.1111/jnc.13987.

# Gemfibrozil, Food and Drug Administration-approved lipid-lowering drug, increases longevity in mouse model of Late Infantile Neuronal Ceroid Lipofuscinosis

**Arunava Ghosh**, **Suresh Babu Rangasamy**, **Khushbu K. Modi**, and **Kalipada Pahan**

Department of Neurological Sciences, Rush University Medical Center, Chicago, USA

## Abstract

Late Infantile Neuronal Ceroid Lipofuscinosis (LINCL) is a rare neurodegenerative disease caused by mutations in the *Cln2* gene that leads to deficiency or loss of function of the tripeptidyl peptidase 1 (TPP1) enzyme. TPP1 deficiency is known to cause the accumulation of autofluoroscent lipid-protein pigments in brain. Similar to other neurodegenerative disorders, LINCL is also associated with neuroinflammation and neuronal damage. Despite investigations, no effective therapy is currently available for LINCL. Therefore, we administered gemfibrozil (gem), an FDA-approved lipid-lowering drug, which has been shown to stimulate lysosomal biogenesis and induce anti-inflammation, orally, at a dose of 7.5 mg/kg body wt/day to *Cln2*$^{(-/-)}$ mice. We observed that gem-fed *Cln2*$^{(-/-)}$ mice lived longer by more than 10 weeks and had better motor activity compared to vehicle (0.1% Methyl cellulose) treatment. Gem treatment lowered the burden of storage materials, increased anti-inflammatory factors like SOCS3 and IL-1Ra, upregulated anti-apoptotic molecule like phospho-Bad, and reduced neuronal apoptosis in the brain of *Cln2*$^{(-/-)}$ mice. Collectively, this study reinforces a neuroprotective role of gem that may be of therapeutic interest in improving the quality of life in LINCL patients.

## Graphical Abstract

We have demonstrated that oral administration of gemfibrozil upregulates the expression of anti-inflammatory molecules like interleukin-1 receptor antagonist (IL-1Ra) and suppressor of cytokine signaling 3 (SOCS3) *in vivo* in the brain of Cln2 null mice, an animal model of late infantile neuronal ceroid lipofuscinosis, leading to the suppression of neuronal apoptosis, increased survival and improved locomotor activity

Corresponding author with complete address: Kalipada Pahan, Ph.D., Department of Neurological Sciences, Rush University Medical Center, 1735 West Harrison St, Suite 310, Chicago, IL 60612, Tel: (312) 563-3592, Fax: (312) 563-3571, Kalipada_Pahan@rush.edu.

**Conflicts of interests**: The authors do not have any conflict of interest.

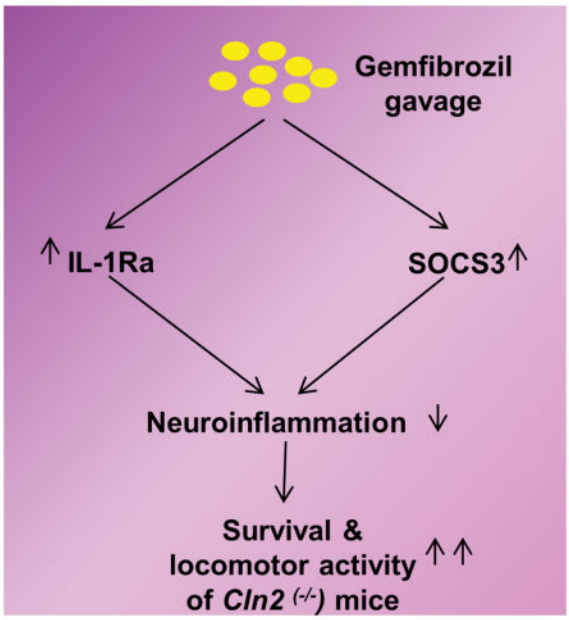


**Keywords**

Batten disease; Mouse model; Longevity; Gemfibrozil; Apoptosis; Anti-inflammation

## Introduction

Lysosomes are membrane bound organelles containing several acid hydrolases that are responsible for degradation of lipid, protein, carbohydrates, and nucleic acids (De Duve & Wattiaux 1966). Defects/deficiencies in almost any of them results in accumulation of undigested/partially digested material in the lysosomes and forms the basis of numerous lysosomal storage disorders (LSDs) (De Duve & Wattiaux 1966, Perez-Sala *et al.* 2009). Late Infantile Neuronal Ceroid Lipofuscinosis (Jansky-Bielschowsky disease, LINCL, Type 2) is one form of NCL that is caused by too mutations in the *Cln2* gene. These mutations lead to deficiency and/or loss of function of tripeptidyl tripeptidase I (TPP-I, a 46 kDa pepstatin insensitive lysosomal protease), resulting in the accumulation of autofluorescent materials in the brain (Sleat *et al.* 1997, Lane *et al.* 1996). LINCL typically produces symptoms at the age of 2–4 years, progresses rapidly and ends in death between ages 8 to 10 as a result of a dramatic decrease in the number of neurons and other cells (Lane et al. 1996, Sleat et al. 1997). Therefore, increasing life span and/or improving the quality of life in patients with LINCL or other NCLs are an important area of research. However, despite years of investigations, no established treatment or drugs are available for this disease; all approaches are merely supportive or symptomatic, indicating an urgent need for novel therapeutic approaches (Chang *et al.* 2008).

Several studies conclude that neuro-inflammation and induction of apoptotic pathways can be attributed to the neuronal damage in most forms of NCL, including LINCL (Geraets *et al.* 2016, Dhar *et al.* 2002, Puranam *et al.* 1997, Kohan *et al.* 2011). Although inflammation is

not the initiating factor in LINCL, glia-mediated sustained inflammatory response is believed to contribute to disease progression (Cooper *et al.* 2015, Macauley *et al.* 2014). Gemfibrozil (gem), an FDA-approved lipid-lowering drug, is known to reduce the level of triglycerides in the blood circulation and decrease the risk of hyperlipidemia (Robins *et al.* 2001, Rubins & Robins 1992, Rubins *et al.* 1999). However, a number of recent studies from us and others reveal that apart from its lipid-lowering effects, gem can also regulate many other signaling pathways responsible for inflammation, switching of T-helper cells, cell-to-cell contact, migration, oxidative stress, and lysosomal biogenesis (Ghosh & Pahan 2012a, Corbett *et al.* 2012, Ghosh *et al.* 2012, Jana *et al.* 2007, Jana & Pahan 2012, Dasgupta *et al.* 2007, Pahan *et al.* 2002, Roy & Pahan 2009, Ghosh *et al.* 2015).

Here, we investigated the therapeutic efficacy of gem in mouse model of LINCL. Behavioral analysis and survival studies on *Cln2*$^{(-/-)}$ mice showed increased longevity and improvement of motor behavior in gem-treated animals compared to vehicle (0.1% methyl cellulose)-treated controls. The burden of storage materials and neuronal apoptosis were also found to be partially reduced in gem-treated animals with increase in levels of phospho-Bad (pBad), an anti-apoptotic molecule. Furthermore, levels of anti-inflammatory factors like SOCS3 and IL-1Ra was found to be elevated in gem-treated animals. Taken together, this study indicates a neuroprotective role of gem in *Cln2*$^{(-/-)}$ animals.

## Materials and Methods

### Reagents and Antibodies

Reagents for TUNEL assay on frozen brain sections were purchased from EMD Millipore (Billerica, MA) and experiments were performed according to manufacturer's protocol. Blocking buffer and secondary antibodies for immune blot (IB) (IRDye 700 or IRDye 800 - labelled) were purchased from Licor (Lincoln, NE). Secondary antibodies for immunohistochemistry (IHC) (FITC or Cy5 – labeled) were purchased from Jackson ImmunoResearch (West Grove, PA). Sources of primary antibodies used in this study along with their applications and dilutions are listed in Table 1.

### Animals

Animal maintaining and experiments were in accordance with National Institute of Health guidelines and were approved by the Institutional Animal Care and Use committee (IACUC) of the Rush University of Medical Center, Chicago, IL. Animals exhibiting mild seizures and tremors were fed and watered through animal feeding needles. However, if any mouse came to the moribund stage, it was decapitated after anesthesia with ketamine/xylazine injectables. Conditions for moribund were as follows: central nervous system disturbance (head tilt, seizures, tremors, circling, spasticity, and paresis); inability to remain upright; evidence of muscle atrophy; chronic diarrhea or constipation; rough coat and distended abdomen; spreading area of alopecia caused by disease; coughing, rales, wheezing and nasal discharge; distinct jaundice and/or paleness (anemia); markedly discolored urine, polyuria or anuria; frank bleeding from any orifice; persistent self-induced trauma.

*Cln2*$^{(+/-)}$ animals were kindly provided by Dr. Peter Lobel (Center for Advanced Biotechnology and Medicine, Robert Wood Johnson Medical School, Piscataway, New Jersey, USA). These animals were inbred and subsequent generations were screened by RT-PCR to further obtain *Cln2*$^{(+/+)}$, *Cln2*$^{(+/-)}$ and *Cln2*$^{(-/-)}$ strains. These *Cln2*$^{(-/-)}$ animals have undetectable TPP1 activity and mimic similar features of human disease including diminished motor behavior, reduced longevity, increased neuropathology in the CNS, and enhanced glial activation (Sleat *et al.* 2004).

### Treatment of Cln2$^{(-/-)}$ mice with gemfibrozil (gem)

Age- and sex-matched *Cln2*$^{(+/+)}$ mice from the same background were used as wild type (WT) controls and *Cln2*$^{(-/-)}$ animals were used in different treatment groups. Gem (7.5mg/kg body wt/day) was dissolved in DMSO followed by dilution in 0.1% methyl cellulose (MeC). *Cln2*$^{(-/-)}$ mice were either not fed (Un – untreated group), gavaged with 0.1% MeC (vehicle treated group) or gavaged with gem (gem-treated group) for 8 weeks for biochemical studies. Similar treatment regimen was followed as long as the animals are not considered to be morbid as described above for survival study. Here, 40 mice (20 male and 20 female) were used per group and animals (4 week old) were randomly selected for any group.

### Locomotor activity

Locomotor activities were measured in *Cln2*$^{(-/-)}$ mice after 8 weeks of gem treatment using Digiscan Monitor (Omnitech Electronics, Inc., Columbus, OH) as described by us (Khasnavis & Pahan 2014, Ghosh *et al.* 2007, Ghosh *et al.* 2009). This Digiscan Monitor records basic locomotion parameters, such as horizontal activity, total distance traveled, movement time, rest time, etc. as well as stereotypy, behavior that is directly controlled by striatum. Briefly, mice were removed directly from their cages and gently placed nose first into a specified corner of the open-field apparatus and after release, data acquisition began every five min interval. DIGISCAN software was used to analyze and store horizontal and vertical activity data, which were monitored automatically by infra-red beams. Here, 12 animals were used per group. After open field tests, six of these mice (n=6) were perfused for immunohistochemical analysis and four mice (n=4) were used for Western blot analysis.

### Immunohistochemistry and cell counting

After 8 weeks of treatment, mice were sacrificed and their brains fixed, embedded, and processed. Sections (30 μm) were made from different brain regions (motor cortex and striatum) using a Leica Cryostat and immunofluorescence staining on fresh frozen sections was performed as described (Corbett *et al.* 2015, Roy *et al.* 2015, Roy *et al.* 2016). Briefly, before adding blocking buffer (2% BSA in PBS), sections were incubated in 100 mM glycine for 20 min for reducing autofluorescence. For details on antibody concentrations, please see Table 1. The samples were mounted and observed under Olympus IX41 fluorescence microscope. Counting analysis was performed using the Olympus Microsuite V software for imaging applications with the help of touch counting module (Corbett et al. 2015, Roy et al. 2015). After acquiring images under 20 X objective lens, images were further analyzed as follows. Before counting cells, the entire image area was calibrated with the help of a rectangular box available in the touch counting panel. Once the area of the

image was measured, touch counting program was applied to count number of fluorescent signals using simple mouse click method. Next, the total number of signals in a given area was divided by the total area of the image and presented as number of cells per square millimeter unit.

### Detection of storage materials

It was performed by monitoring subunit c of mitochondrial ATP synthase (SCMAS) by immunofluorescence. Please see Table 1 for details on antibody dilutions. DAPI was used to monitor nucleus. SCMAS-associated fluorescence intensity was quantified by using the Olympus Microsuite V software. Briefly, captured images were opened in the infinity image viewer and the contour was drawn around the granules to obtain the fluorescence intensity.

### Immunoblot analysis

After 8 weeks of treatment, mice were sacrificed and cortex and striatum regions were isolated, homogenized in RIPA buffer (150 mM sodium chloride, 1.0% NP-40 or Triton X-100, 0.5% sodium deoxycholate, 0.1% SDS (sodium dodecyl sulphate), 50 mM Tris, pH 8.0), supernatant was taken and protein was estimated by BioRad protein assay. Equal amounts of protein from the tissue extract were separated in 12% or 15% Bis-Tris gels and proteins were transferred onto a nitrocellulose membrane (Bio-Rad) using the Thermo-Pierce Fast Semi-Dry Blotter (Corbett et al. 2015, Roy et al. 2015, Roy et al. 2016). The membrane was then washed for 15 min in TBS plus Tween 20 (TBST) and blocked for 1 h in TBST containing BSA. Next, membranes were incubated overnight at 4°C under shaking conditions with the antibodies for the following proteins: β-Actin, IL-1Ra, phospho-Bad, and SOCS3. Please see Table 1 for details on antibody dilutions. The next day, membranes were washed in TBST for 1 h, incubated in secondary antibodies against primary antibody hosts (all 1:10,000; Jackson ImmunoResearch) for 1 h, washed for one more h and visualized under the Odyssey® Infrared Imaging System (Li-COR, Lincoln, NE).

### Statistical analysis

All values are expressed as means ± SEM. One-way ANOVA followed by Tukey's or Scheffé's post hoc tests, Student's *t* tests and Kaplan–Meier survival estimators ($\chi^2$) were used for data analyses, using SPSS 19.

## Results

### Gem treatment prolongs the lifespan in *Cln2*$^{(-/-)}$ mice

*Cln2*$^{(-/-)}$ mouse serves as an important animal model for testing new therapeutic approaches against LINCL (Cabrera-Salazar *et al.* 2007, Sleat *et al.* 2008, Chang et al. 2008, Sleat et al. 2004). Usually, LINCL progresses rapidly, ending in death between ages 8 and 10 (Sohar *et al.* 1999, Sleat et al. 1997). Similarly, *Cln2*$^{(-/-)}$ mice also die within 140 d (Sleat et al. 2004). Therefore, at first, we examined whether oral gem treatment was capable of increasing the lifespan of *Cln2*$^{(-/-)}$ mice. Earlier we have demonstrated that after oral administration, gem enters into the CNS (Dasgupta et al. 2007). Mice were treated daily with gem (7.5 mg/kg body weight/day) via gavage from 4 weeks of age. Since gem was solubilized in 0.1% methyl cellulose, one group of *Cln2*$^{(-/-)}$ mice also received 0.1% methyl

cellulose as vehicle. Untreated *Cln2*$^{(-/-)}$ male and female mice started dying from 95 days and within 137 days, all *Cln2*$^{(-/-)}$ mice died (Fig. 1A). In terms of survival, we did not see any difference between male and female *Cln2*$^{(-/-)}$ mice. However, gem-treated *Cln2*$^{(-/-)}$ mice survived until 204 days, suggesting that gem is capable of increasing the lifespan of *Cln2*$^{(-/-)}$ mice by more than 2 months (Fig. 1A). On the other hand, all vehicle-treated mice died within 150 days (Fig. 1A), suggesting very mild protection by vehicle only. These results are also supported by mean survival days of each group of mice (Fig. 1B).

## Gem treatment improves motor behavior in *Cln2*$^{(-/-)}$ mice

Together with increase in longevity, another therapeutic goal of neuroprotection for LINCL patients is to decrease functional impairment. Therefore, to examine whether gem increases not only longevity but also improves motor behavior in *Cln2*$^{(-/-)}$ mice, we monitored locomotor activities. Locomotor activities were monitored 8 weeks after gem treatment. *Cln2*$^{(-/-)}$ mice exhibited marked decrease in horizontal activity (Fig. 2A), movement time (Fig. 2B), number of movement (Fig. 2C), total distance traveled (Fig. 2D), and stereotypy counts (Fig. 2E) as compared to WT mice. On the other hand, the rest time was more in *Cln2*$^{(-/-)}$ mice than WT mice (Fig. 2F). However, oral administration of gem significantly improved locomotor activities in *Cln2*$^{(-/-)}$ mice (Fig. 2A–F).

## Gem treatment lowers the burden of storage material in the brain of *Cln2*$^{(-/-)}$ mice

One of the common characteristics of lysosomal storage disorders including LINCL is the accumulation of autofluorescent inclusion bodies in all tissues including the brain (Boustany 2013, Hachiya *et al.* 2006). Recently we delineated that gemfibrozil is capable of stimulating lysosomal biogenesis via PPARα-mediated transcriptional upregulation of TFEB (Ghosh et al. 2015). Since gem treatment prolongs the lifespan and improves the motor behavior of *Cln2*$^{(-/-)}$ mice, we examined whether gem treatment could reduce the load of storage material *in vivo* in the motor cortex. As expected, we observed marked increase in subunit c of mitochondrial ATP synthase (SCMAS) accumulation in the motor cortex of *Cln2*$^{(-/-)}$ mice as compared to WT mice (Fig. 3A–B). However, gem treatment of *Cln2*$^{(-/-)}$ mice led to significant decrease in SCMAS (Fig. 3A–B). These results were specific as vehicle treatment did not result in such decrease in storage materials (Fig. 3A–B).

## Gem treatment prevents neuronal apoptosis in the brain of *Cln2*$^{(-/-)}$ mice

As seen in other neurodegenerative disorders (Cotman & Anderson 1995, Saha & Pahan 2006), apoptosis is also responsible for neuronal degeneration in LINCL (Dhar et al. 2002, Puranam et al. 1997, Lane et al. 1996). Therefore, we examined whether gem treatment was capable of suppressing neuronal apoptosis in the CNS of *Cln2*$^{(-/-)}$ mice. It is evident from Figure 4A–B that NeuN-positive neurons underwent apoptosis in the motor cortex of *Cln2*$^{(-/-)}$ mice. However, oral treatment of gem strongly inhibited neuronal apoptosis *in vivo* in the motor cortex (Fig. 4A–B). These results are specific as vehicle (0.1% methyl cellulose) treatment did not suppress neuronal apoptosis (Fig. 4A–B). Although BAD is an apoptotic molecule, phosphorylation of BAD is known to support cell survival (Datta *et al.* 1999, Datta *et al.* 2002). Therefore, we examined the level of phospho-BAD (P-BAD) in the motor cortex of *Cln2*$^{(-/-)}$ mice. Consistent to increased apoptosis, the level of P-BAD decreased in the motor cortex of *Cln2*$^{(-/-)}$ mice (Fig. 4C–D). However, treatment of

*Cln2*$^{(-/-)}$ mice with gem, but not vehicle, led to upregulation of P-BAD (Fig. 4C–D). To understand whether the effect of gem is confined to motor cortex or other part of the brain is also benefitted by gem treatment, we monitored apoptosis in striatum. Similar to motor cortex, we also observed increase in apoptosis (Fig. 5A–B) and decrease in P-BAD (Fig. 5C–D) in the striatum of *Cln2*$^{(-/-)}$ mice. However, gem treatment reduced neuronal apoptosis (Fig. 5A–B) and increased the level of P-BAD (Fig. 5C–D) *in vivo* in the striatum, suggesting that oral gem treatment is capable of suppressing apoptosis in different parts of the brain of *Cln2*$^{(-/-)}$ mice.

### Gem increases the levels of anti-inflammatory factors in the brain of *Cln2*$^{(-/-)}$ mice

We have demonstrated that gem is anti-inflammatory (Jana & Pahan 2012, Jana et al. 2007, Pahan et al. 2002) and that gem increases the level of SOCS3 and IL-1Ra, anti-inflammatory factors, in different brain cells (Corbett et al. 2012, Ghosh & Pahan 2012b). Therefore, here, we investigated whether gem treatment could upregulate these anti-inflammatory molecules *in vivo* in the brain of *Cln2*$^{(-/-)}$ mice. At 12 weeks of age, we observed decrease in SOCS3 and IL-1Ra in motor cortex (Fig. 6A–C) and striatum (Fig. 6D–F) of *Cln2*$^{(-/-)}$ mice as compared to age-matched WT mice. However, after 8 weeks of oral treatment with gem, but not vehicle, the increase in SOCS3 (Fig. 6A, B, D, & E) and IL-1Ra (Fig. 6A, D, C, & F) was seen in both motor cortex and striatum of *Cln2*$^{(-/-)}$ mice. To confirm these findings further, next, we performed double-label immunofluorescence in striatal sections. Although we observed more astroglia (Fig. 7A) and microglia (Fig. 7B) in striatal sections of *Cln2*$^{(-/-)}$ mice as compared to WT mice, there was a loss of SOCS3 in the former as compared to the latter (Fig. 7A–C). However, similar to Western blot results, marked increase in SOCS3 was seen in the striatum of *Cln2*$^{(-/-)}$ mice after gem treatment (Fig. 7A–C). This increase in SOCS3 was visible in astrocytes (Fig. 7A & D), microglia (Fig. 7B & E) as well as other brain cells (Fig. 7). Similar to SOCS3, we also noticed the loss of IL-1Ra in the striatum of *Cln2*$^{(-/-)}$ mice as compared to WT mice (Fig. 8A–E). However, treatment of *Cln2*$^{(-/-)}$ mice with gem, but not vehicle, led to restoration and/or upregulation of IL-1Ra in the striatum (Fig, 8A–E). Again, gem-induced increase in IL-1Ra *in vivo* in the striatum of *Cln2*$^{(-/-)}$ mice was in both astrocytes (Fig. 8A & D) and microglia (Fig. 8B & E). Interestingly, in both motor cortex and striatum of *Cln2*$^{(-/-)}$ mice, we did not observe any reduction in either astroglia or microglia after gem treatment (Figs. 7 & 8), suggesting that once astrogliosis or microgliosis occurs *in vivo* in the brain of a chronic neurodegenerating condition as found in *Cln2*$^{(-/-)}$ mice, gemfibrozil treatment may only modulate their function towards the anti-inflammatory mode without decreasing its number.

## Discussion

Mutations in the *Cln2* result in deficiency and/or loss of function of the TPP1 enzyme, ultimately causing LINCL (Bellettato & Scarpa 2010, Walus *et al.* 2010, Sohar et al. 1999). Although enzyme replacement therapy and gene therapy clinical trials are ongoing, no established drug mediated therapy is currently available for LINCL. Therefore, development of neuroprotective therapeutic approaches for delaying the disease progression, improving locomotor functions and increasing the survival of LINCL patients are of paramount importance. *Cln2*$^{(-/-)}$ mouse is useful in determining new therapeutic strategies and testing

the efficacy of new drugs for LINCL. Here, we demonstrate for the first time that gemfibrozil (gem), an FDA-approved drug for hyperlipidemia in humans, improves locomotor functions and prolongs the lifespan in *Cln2*$^{(-/-)}$ mice. Recently we have delineated that gemfibrozil is capable of upregulating TPP1 in cultured mouse and human brain cells and *in vivo* in mouse brain via PPARα/RXRα pathway (Ghosh et al. 2012). However, there is no TPP1 in *Cln2*$^{(-/-)}$ mice. Therefore, in this case, gem is employing TPP1-independent mechanisms to delay the disease progression in *Cln2*$^{(-/-)}$ mice.

Although the importance of autofluorescent storage materials in the pathogenesis of LSDs including LINCL is not known, these inclusion bodies are one of hallmarks of LSDs (Boustany 2013). Recently we have also demonstrated that gem is capable of stimulating lysosomal biogenesis via PPARα-mediated transcriptional activation of TFEB (Ghosh et al. 2015), suggesting possible lowering of storage materials by gem treatment. Accordingly, gem was able to reduce storage materials from the motor cortex of *Cln2*$^{(-/-)}$ mice. Therefore, even in the absence of TPP1 (a vital enzyme in the degradation pathway), gem can stimulate autophagic clearance via TFEB-mediated activation of other lysosomal enzymes. Earlier we have demonstrated that in skin fibroblasts of patients with LINCL, a combination of gemfibrozil and retinoic acid increased lysosomal biogenesis irrespective of the disease status (Ghosh et al. 2015).

Neuronal apoptosis is a hallmark of most of the known neurodegenerative diseases including lysosomal storage disorders (Dhar et al. 2002, Puranam et al. 1997, Lane et al. 1996). Strong inhibition of neuronal apoptosis in different parts of the CNS of *Cln2*$^{(-/-)}$ mice by gem suggests that this anti-apoptotic property of gem may contribute to its lifespan-prolonging efficacy in these mice. BAD, a member of the BCL-2 family, is an important regulator of apoptosis (Datta et al. 1999, Datta et al. 2002). Non-phosphorylated form BAD is known to induce apoptosis by forming heterodimers with survival proteins Bcl-x and Bcl-2, thereby allowing two other pro-apoptotic proteins, BAK and BAX, to aggregate and induce release of cytochrome c (Datta et al. 1999, Datta et al. 2002). On the other hand, phosphorylated BAD is sequestered in the cytoplasm by binding to 14-3-3 and thereby allowing cell survival. Here, we have demonstrated that gem treatment restores/upregulates the level of P-BAD in motor cortex and striatum of *Cln2*$^{(-/-)}$ mice. Signaling mechanisms leading to phosphorylation of BAD is becoming clear. Phosphatidylinositol-3 kinase (PI3K) is a key signaling molecule implicated in the regulation of a broad array of biological responses including cell survival (Koyasu 2003). Several studies have shown that activation of PI3K leads to phosphorylation of BAD via Akt (Ellert-Miklaszewska *et al.* 2005, Li *et al.* 2001). Interestingly, gem induces the activation of p85α-associated type IA PI3K in brain cells (Jana et al. 2007). Therefore, it is possible that gem suppresses apoptosis in the CNS of *Cln2*$^{(-/-)}$ mice via PI3K – (P)BAD pathway.

Although there are many causes of apoptosis in the CNS, neuroinflammation is an important one. Therefore, chronic inflammation mediated by activated glial cells is becoming a hallmark of several neurodegenerative disorders including LINCL (Shyng & Sands 2014, Cooper et al. 2015, Macauley et al. 2014). IL-1β, a proinflammatory cytokine, is implicated in the pathogenesis of neurodegenerative diseases. Although IL-1β binds to its high-affinity receptor, IL-1R, and upregulates proinflammatory signaling pathways, IL-1R antagonist

(IL-1Ra) adheres to the same receptor and inhibits proinflammatory cell signaling (Basu *et al.* 2004). Similarly, suppressor of cytokine signaling (SOCS) proteins also play a crucial role in inhibiting cytokine signaling and inflammatory gene expression in various cell types, including glial cells (Baker *et al.* 2009, Chen *et al.* 2000). Therefore, upregulation of IL-1Ra and SOCS is considered important in attenuating inflammation. Recently, we have seen that gem upregulates SOCS3 in glial cells via PI3K-mediated activation of KLF4 (Ghosh & Pahan 2012b) and that gem increases IL-1Ra via PI3K-mediated activation of CREB (Corbett et al. 2012). It is important to see that gem treatment increased the level of both SOCS3 and IL-1Ra in striatum and cortex of *Cln2*$^{(-/-)}$ mice. Therefore, by upregulating these important anti-inflammatory molecules, gem may exhibit protection and delay the disease onset in *Cln2*$^{(-/-)}$ mice.

Gem has several advantages over other prospective neuroprotective agents. For example, gem is an oral drug and fairly nontoxic (Backes *et al.* 2007, Roy & Pahan 2009, Pahan 2006). It has been well tolerated in human and animal studies. Known as ‘Lopid’ in the pharmacy, it is a commonly used lipid-lowering drug in humans since FDA approval in 1981. The Veterans Affairs High-Density Lipoprotein Intervention Trial (VA-HIT) has reported that coronary heart disease events are significantly reduced by gem in patients when the predominant lipid abnormality was low HDL-C (Robins et al. 2001). In a double-blind, randomized, placebo-controlled trial, this drug was shown to reduce small low-density lipoprotein more in normolipemic subjects classified as low-density lipoprotein pattern B compared with pattern A (Superko *et al.* 2005). Another recent trial showed that low-density lipoprotein and HDL particle subclasses are favorably changed by gem therapy (Otvos *et al.* 2006). Gem also lowers triglycerides and raises HDL with reasonable safety in a pediatric population with metabolic syndrome (Smalley & Goldberg 2008).

In summary, we have demonstrated that gemfibrozil, an FDA-approved lipid-lowering drug in humans, reduces storage materials, upregulates anti-inflammatory molecules, suppresses neuronal apoptosis, and increases the lifespan of *Cln2*$^{(-/-)}$ mice. Although *in vivo* situation of *Cln2*$^{(-/-)}$ mouse brain and its treatment with gem may not truly resemble the *in vivo* neurodegenerative situation in patients with LINCL, our results identify gem as a possible therapeutic agent to prolong the lifespan in LINCL patients.

## Acknowledgments

This study was supported by the National Institutes of Health (AG050431), Noah’s Hope Foundation, Hope 4 Bridget, Fighting for Maya, and Harmony 4 Hope.

## Abbreviations

| | |
|---|---|
| **LINCL** | Late Infantile Neuronal Ceroid Lipofuscinosis |
| **TPP-I** | tripeptidyl tripeptidase I |
| **SOCS** | suppressor of cytokine signaling |
| **IL-1Ra** | Interleukin-1β receptor antagonist |
| **gem** | Gemfibrozil |

**MeC** methyl cellulose

## References


Backes JM, Gibson CA, Ruisinger JF, Moriarty PM. Fibrates: what have we learned in the past 40 years? Pharmacotherapy. 2007; 27:412–424. [PubMed: 17316152]

Baker BJ, Akhtar LN, Benveniste EN. SOCS1 and SOCS3 in the control of CNS immunity. Trends Immunol. 2009; 30:392–400. [PubMed: 19643666]

Basu A, Krady JK, Levison SW. Interleukin-1: a master regulator of neuroinflammation. J Neurosci Res. 2004; 78:151–156. [PubMed: 15378607]

Bellettato CM, Scarpa M. Pathophysiology of neuropathic lysosomal storage disorders. J Inherit Metab Dis. 2010; 33:347–362. [PubMed: 20429032]

Boustany RM. Lysosomal storage diseases--the horizon expands. Nat Rev Neurol. 2013; 9:583–598. [PubMed: 23938739]

Cabrera-Salazar MA, Roskelley EM, Bu J, et al. Timing of therapeutic intervention determines functional and survival outcomes in a mouse model of late infantile batten disease. Mol Ther. 2007; 15:1782–1788. [PubMed: 17637720]

Chang M, Cooper JD, Sleat DE, Cheng SH, Dodge JC, Passini MA, Lobel P, Davidson BL. Intraventricular enzyme replacement improves disease phenotypes in a mouse model of late infantile neuronal ceroid lipofuscinosis. Mol Ther. 2008; 16:649–656. [PubMed: 18362923]

Chen XP, Losman JA, Rothman P. SOCS proteins, regulators of intracellular signaling. Immunity. 2000; 13:287–290. [PubMed: 11021526]

Cooper JD, Tarczyluk MA, Nelvagal HR. Towards a new understanding of NCL pathogenesis. Biochim Biophys Acta. 2015; 1852:2256–2261. [PubMed: 26026924]

Corbett GT, Gonzalez FJ, Pahan K. Activation of peroxisome proliferator-activated receptor alpha stimulates ADAM10-mediated proteolysis of APP. Proc Natl Acad Sci U S A. 2015; 112:8445–8450. [PubMed: 26080426]

Corbett GT, Roy A, Pahan K. Gemfibrozil, a Lipid-Lowering Drug, Upregulates IL-1 Receptor Antagonist in Mouse Cortical Neurons: Implications for Neuronal Self-Defense. J Immunol. 2012; 189:1002–1013. [PubMed: 22706077]

Cotman CW, Anderson AJ. A potential role for apoptosis in neurodegeneration and Alzheimer's disease. Mol Neurobiol. 1995; 10:19–45. [PubMed: 7598831]

Dasgupta S, Roy A, Jana M, Hartley DM, Pahan K. Gemfibrozil ameliorates relapsing-remitting experimental autoimmune encephalomyelitis independent of peroxisome proliferator-activated receptor-alpha. Mol Pharmacol. 2007; 72:934–946. [PubMed: 17625103]

Datta SR, Brunet A, Greenberg ME. Cellular survival: a play in three Akts. Genes Dev. 1999; 13:2905–2927. [PubMed: 10579998]

Datta SR, Ranger AM, Lin MZ, Sturgill JF, Ma YC, Cowan CW, Dikkes P, Korsmeyer SJ, Greenberg ME. Survival factor-mediated BAD phosphorylation raises the mitochondrial threshold for apoptosis. Dev Cell. 2002; 3:631–643. [PubMed: 12431371]

De Duve C, Wattiaux R. Functions of lysosomes. Annu Rev Physiol. 1966; 28:435–492. [PubMed: 5322983]

Dhar S, Bitting RL, Rylova SN, Jansen PJ, Lockhart E, Koeberl DD, Amalfitano A, Boustany RM. Flupirtine blocks apoptosis in batten patient lymphoblasts and in human postmitotic CLN3- and CLN2-deficient neurons. Ann Neurol. 2002; 51:448–466. [PubMed: 11921051]

Ellert-Miklaszewska A, Kaminska B, Konarska L. Cannabinoids down-regulate PI3K/Akt and Erk signalling pathways and activate proapoptotic function of Bad protein. Cell Signal. 2005; 17:25–37. [PubMed: 15451022]

Geraets RD, Koh S, Hastings ML, Kielian T, Pearce DA, Weimer JM. Moving towards effective therapeutic strategies for Neuronal Ceroid Lipofuscinosis. Orphanet J Rare Dis. 2016; 11:40. [PubMed: 27083890]

Ghosh A, Corbett GT, Gonzalez FJ, Pahan K. Gemfibrozil and fenofibrate, Food and Drug Administration-approved lipid-lowering drugs, up-regulate tripeptidyl-peptidase 1 in brain cells

via peroxisome proliferator-activated receptor alpha: implications for late infantile Batten disease therapy. J Biol Chem. 2012; 287:38922–38935. [PubMed: 22989886]

Ghosh A, Jana M, Modi K, Gonzalez FJ, Sims KB, Berry-Kravis E, Pahan K. Activation of peroxisome proliferator-activated receptor alpha induces lysosomal biogenesis in brain cells: implications for lysosomal storage disorders. J Biol Chem. 2015; 290:10309–10324. [PubMed: 25750174]

Ghosh A, Pahan K. Gemfibrozil, a lipid-lowering drug, induces suppressor of cytokine signaling 3 in glial cells: implications for neurodegenerative disorders. J Biol Chem. 2012a; 287:27189–27203. [PubMed: 22685291]

Ghosh A, Pahan K. Gemfibrozil, a lipid-lowering drug, induces suppressor of cytokine signaling 3 in glial cells: Implications for neurodegenerative disorders. J Biol Chem. 2012b

Ghosh A, Roy A, Liu X, et al. Selective inhibition of NF-kappaB activation prevents dopaminergic neuronal loss in a mouse model of Parkinson's disease. Proc Natl Acad Sci U S A. 2007; 104:18754–18759. [PubMed: 18000063]

Ghosh A, Roy A, Matras J, Brahmachari S, Gendelman HE, Pahan K. Simvastatin inhibits the activation of p21ras and prevents the loss of dopaminergic neurons in a mouse model of Parkinson's disease. J Neurosci. 2009; 29:13543–13556. [PubMed: 19864567]

Hachiya Y, Hayashi M, Kumada S, Uchiyama A, Tsuchiya K, Kurata K. Mechanisms of neurodegeneration in neuronal ceroid-lipofuscinoses. Acta Neuropathol. 2006; 111:168–177. [PubMed: 16465529]

Jana M, Jana A, Liu X, Ghosh S, Pahan K. Involvement of phosphatidylinositol 3-kinase-mediated up-regulation of I kappa B alpha in anti-inflammatory effect of gemfibrozil in microglia. J Immunol. 2007; 179:4142–4152. [PubMed: 17785853]

Jana M, Pahan K. Gemfibrozil, a lipid lowering drug, inhibits the activation of primary human microglia via peroxisome proliferator-activated receptor beta. Neurochem Res. 2012; 37:1718–1729. [PubMed: 22528839]

Khasnavis S, Pahan K. Cinnamon treatment upregulates neuroprotective proteins Parkin and DJ-1 and protects dopaminergic neurons in a mouse model of Parkinson's disease. J Neuroimmune Pharmacol. 2014; 9:569–581. [PubMed: 24946862]

Kohan R, Cismondi IA, Oller-Ramirez AM, Guelbert N, Anzolini TV, Alonso G, Mole SE, de Kremer DR, de Halac NI. Therapeutic approaches to the challenge of neuronal ceroid lipofuscinoses. Curr Pharm Biotechnol. 2011; 12:867–883. [PubMed: 21235444]

Koyasu S. The role of PI3K in immune cells. Nat Immunol. 2003; 4:313–319. [PubMed: 12660731]

Lane SC, Jolly RD, Schmechel DE, Alroy J, Boustany RM. Apoptosis as the mechanism of neurodegeneration in Batten's disease. J Neurochem. 1996; 67:677–683. [PubMed: 8764595]

Li Y, Tennekoon GI, Birnbaum M, Marchionni MA, Rutkowski JL. Neuregulin signaling through a PI3K/Akt/Bad pathway in Schwann cell survival. Mol Cell Neurosci. 2001; 17:761–767. [PubMed: 11312610]

Macauley SL, Wong AM, Shyng C, et al. An anti-neuroinflammatory that targets dysregulated glia enhances the efficacy of CNS-directed gene therapy in murine infantile neuronal ceroid lipofuscinosis. J Neurosci. 2014; 34:13077–13082. [PubMed: 25253854]

Otvos JD, Collins D, Freedman DS, Shalaurova I, Schaefer EJ, McNamara JR, Bloomfield HE, Robins SJ. Low-density lipoprotein and high-density lipoprotein particle subclasses predict coronary events and are favorably changed by gemfibrozil therapy in the Veterans Affairs High-Density Lipoprotein Intervention Trial. Circulation. 2006; 113:1556–1563. [PubMed: 16534013]

Pahan K. Lipid-lowering drugs. Cell Mol Life Sci. 2006; 63:1165–1178. [PubMed: 16568248]

Pahan K, Jana M, Liu X, Taylor BS, Wood C, Fischer SM. Gemfibrozil, a lipid-lowering drug, inhibits the induction of nitric-oxide synthase in human astrocytes. J Biol Chem. 2002; 277:45984–45991. [PubMed: 12244038]

Perez-Sala D, Boya P, Ramos I, Herrera M, Stamatakis K. The C-terminal sequence of RhoB directs protein degradation through an endo-lysosomal pathway. PLoS One. 2009; 4:e8117. [PubMed: 19956591]

Puranam K, Qian WH, Nikbakht K, Venable M, Obeid L, Hannun Y, Boustany RM. Upregulation of Bcl-2 and elevation of ceramide in Batten disease. Neuropediatrics. 1997; 28:37–41. [PubMed: 9151319]

Robins SJ, Collins D, Wittes JT, et al. Relation of gemfibrozil treatment and lipid levels with major coronary events: VA-HIT: a randomized controlled trial. JAMA. 2001; 285:1585–1591. [PubMed: 11268266]

Roy A, Jana M, Kundu M, Corbett GT, Rangaswamy SB, Mishra RK, Luan CH, Gonzalez FJ, Pahan K. HMG-CoA Reductase Inhibitors Bind to PPARalpha to Upregulate Neurotrophin Expression in the Brain and Improve Memory in Mice. Cell Metab. 2015; 22:253–265. [PubMed: 26118928]

Roy A, Kundu M, Jana M, Mishra RK, Yung Y, Luan CH, Gonzalez FJ, Pahan K. Identification and characterization of PPARalpha ligands in the hippocampus. Nat Chem Biol. 2016; 12:1075–1083. [PubMed: 27748752]

Roy A, Pahan K. Gemfibrozil, stretching arms beyond lipid lowering. Immunopharmacol Immunotoxicol. 2009; 31:339–351. [PubMed: 19694602]

Rubins HB, Robins SJ. Effect of reduction of plasma triglycerides with gemfibrozil on high-density-lipoprotein-cholesterol concentrations. J Intern Med. 1992; 231:421–426. [PubMed: 1588269]

Rubins HB, Robins SJ, Collins D, et al. Gemfibrozil for the secondary prevention of coronary heart disease in men with low levels of high-density lipoprotein cholesterol. Veterans Affairs High-Density Lipoprotein Cholesterol Intervention Trial Study Group. N Engl J Med. 1999; 341:410–418. [PubMed: 10438259]

Saha RN, Pahan K. HATs and HDACs in neurodegeneration: a tale of disconcerted acetylation homeostasis. Cell Death Differ. 2006; 13:539–550. [PubMed: 16167067]

Shyng C, Sands MS. Astrocytosis in infantile neuronal ceroid lipofuscinosis: friend or foe? Biochem Soc Trans. 2014; 42:1282–1285. [PubMed: 25233404]

Sleat DE, Donnelly RJ, Lackland H, Liu CG, Sohar I, Pullarkat RK, Lobel P. Association of mutations in a lysosomal protein with classical late-infantile neuronal ceroid lipofuscinosis. Science. 1997; 277:1802–1805. [PubMed: 9295267]

Sleat DE, El-Banna M, Sohar I, Kim KH, Dobrenis K, Walkley SU, Lobel P. Residual levels of tripeptidyl-peptidase I activity dramatically ameliorate disease in late-infantile neuronal ceroid lipofuscinosis. Mol Genet Metab. 2008; 94:222–233. [PubMed: 18343701]

Sleat DE, Wiseman JA, El-Banna M, et al. A mouse model of classical late-infantile neuronal ceroid lipofuscinosis based on targeted disruption of the CLN2 gene results in a loss of tripeptidyl-peptidase I activity and progressive neurodegeneration. J Neurosci. 2004; 24:9117–9126. [PubMed: 15483130]

Smalley CM, Goldberg SJ. A pilot study in the efficacy and safety of gemfibrozil in a pediatric population. J Clin Lipidol. 2008; 2:106–111. [PubMed: 21291726]

Sohar I, Sleat DE, Jadot M, Lobel P. Biochemical characterization of a lysosomal protease deficient in classical late infantile neuronal ceroid lipofuscinosis (LINCL) and development of an enzyme-based assay for diagnosis and exclusion of LINCL in human specimens and animal models. J Neurochem. 1999; 73:700–711. [PubMed: 10428067]

Superko HR, Berneis KK, Williams PT, Rizzo M, Wood PD. Gemfibrozil reduces small low-density lipoprotein more in normolipemic subjects classified as low-density lipoprotein pattern B compared with pattern A. Am J Cardiol. 2005; 96:1266–1272. [PubMed: 16253595]

Walus M, Kida E, Golabek AA. Functional consequences and rescue potential of pathogenic missense mutations in tripeptidyl peptidase I. Hum Mutat. 2010; 31:710–721. [PubMed: 20340139]

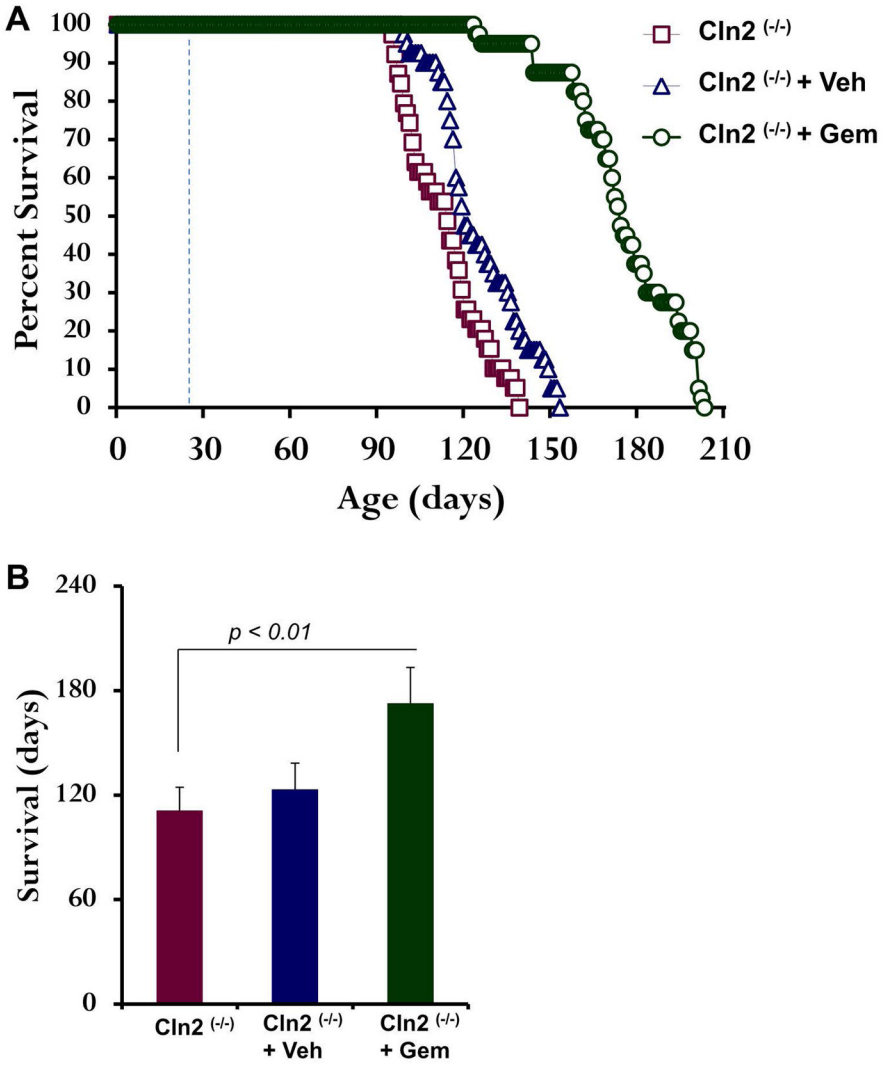


**Figure 1. Gemfibrozil (gem) prolongs the life span of *Cln2* $^{(-/-)}$ mice**

*Cln2* $^{(-/-)}$ animals were treated with gem (dissolved in 0.1% MeC) orally at a dose of 7.5 mg/kg body weight/day. Treatment started from 4 weeks of age for all groups. One group of animals received only MeC as vehicle. A) Percentage of survival is shown by Kaplan–Meier plot. B) Mean survival days are shown for all three groups. Forty mice (n=40) containing 20 males and 20 female were used in each group.

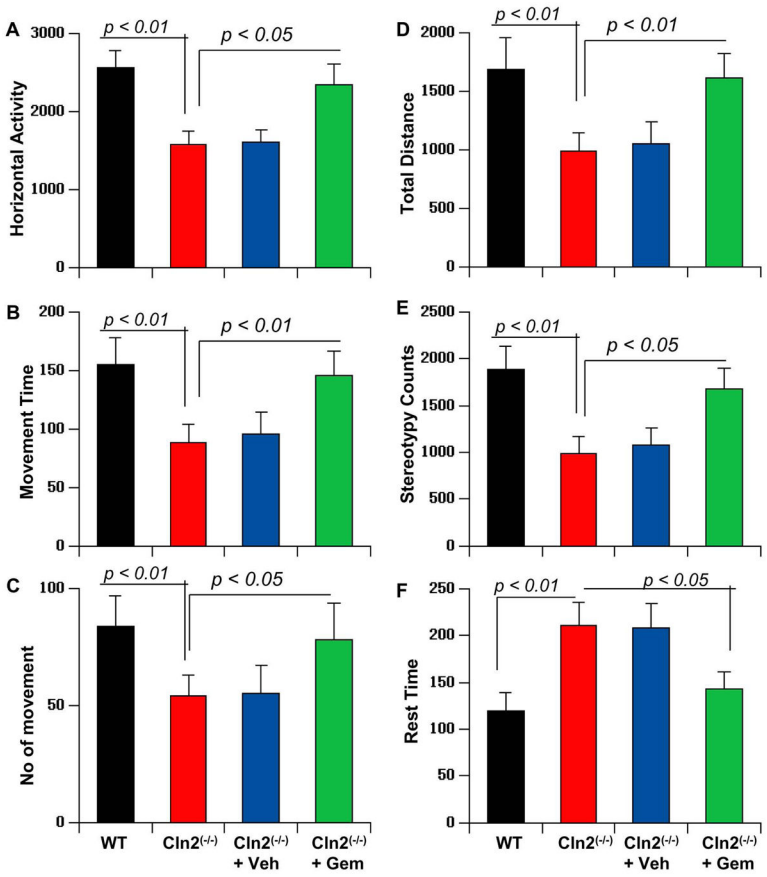


**Figure 2. Gem treatment delays the loss of motor activity in *Cln2* $^{(-/-)}$ mice**

*Cln2* $^{(-/-)}$ animals (4 weeks old) were treated with gem (dissolved in 0.1% MeC) orally at a dose of 7.5 mg/kg body weight/day. After 8 weeks of treatment, mice were monitored for horizontal activity (A), movement time (B), number of movement (C), total distance travelled (D), stereotypy counts (E), and rest time (F). *Cln2* $^{(-/-)}$ mice receiving only vehicle and background-matched wild type (WT) mice were also run for comparison. Results represent mean ± SEM of twelve mice (n=12) per group. Male and female mice were kept in each group in equal ratio.

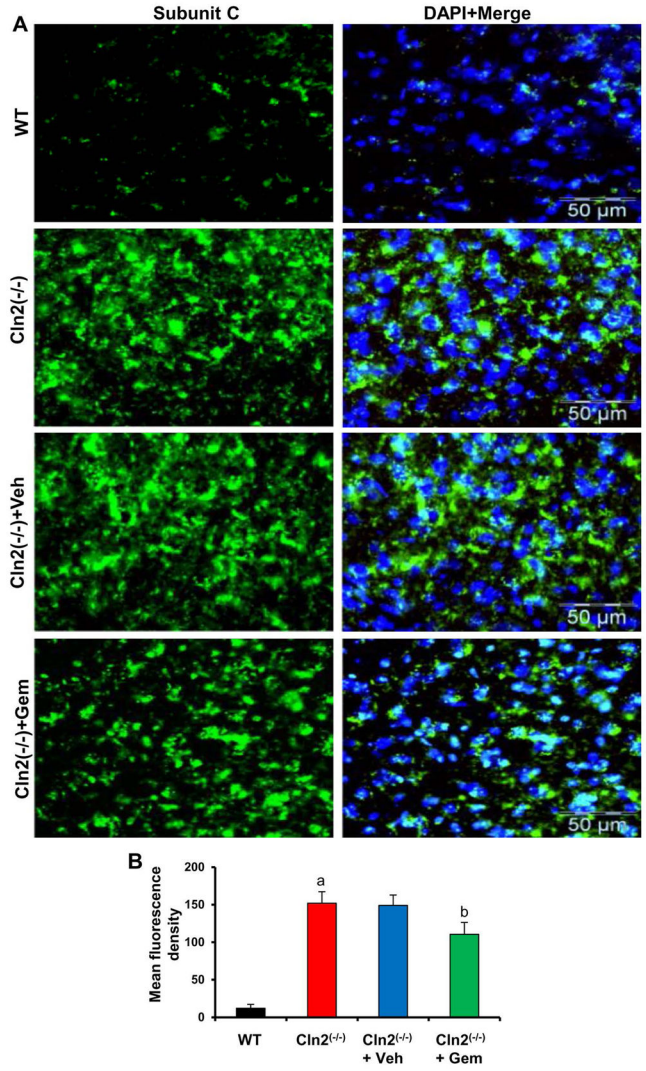


**Figure 3. Gem treatment reduces storage materials *in vivo* in the motor cortex of *Cln2* $^{(-/-)}$ mice**

*Cln2* $^{(-/-)}$ animals (4 weeks old) were treated with gem (dissolved in 0.1% MeC) orally at a dose of 7.5 mg/kg body weight/day. After 8 weeks of treatment, storage pigments were observed in cortical sections by immunofluorescence analysis of subunit C (A). DAPI was used to visualize nucleus. B) Subunit C positive immunofluorescence was quantified in two different sections (two images per section) of each of six different mice (n=6) per group using NIH Image J software as described under Methods section. $^{a}p < 0.001$ *vs WT-control;* $^{b}p < 0.05$ *vs Cln2* $^{(-/-)}$.

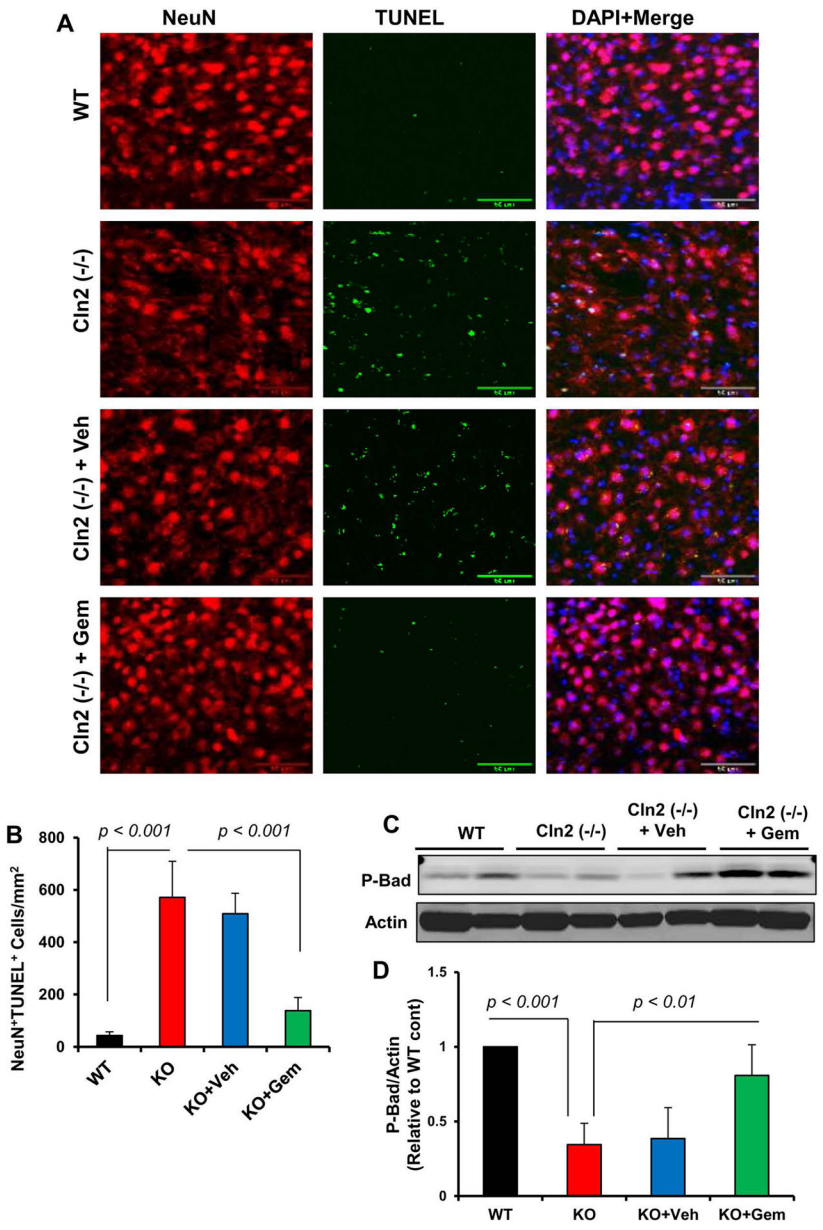


**Figure 4. Gem treatment attenuates apoptosis *in vivo* in the motor cortex of *Cln2* $^{(-/-)}$ mice**

*Cln2* $^{(-/-)}$ animals (4 weeks old) were treated with gem (dissolved in 0.1% MeC) orally at a dose of 7.5 mg/kg body weight/day. After 8 weeks of treatment, cortical sections (immediately dorsal to CA1 hippocampal region) were double-labeled for NeuN and TUNEL (A). $NeuN^{+}TUNEL^{+}$ cells were counted (B) in two different cortical sections of each of six different mice (n=6) per group. C) Cortical homogenates were immunoblotted for phospho-BAD. Actin was run as loading control. D) Bands were scanned and values (P-BAD/Actin) are presented as relative to WT control. Results are mean ± SEM of four mice per group.

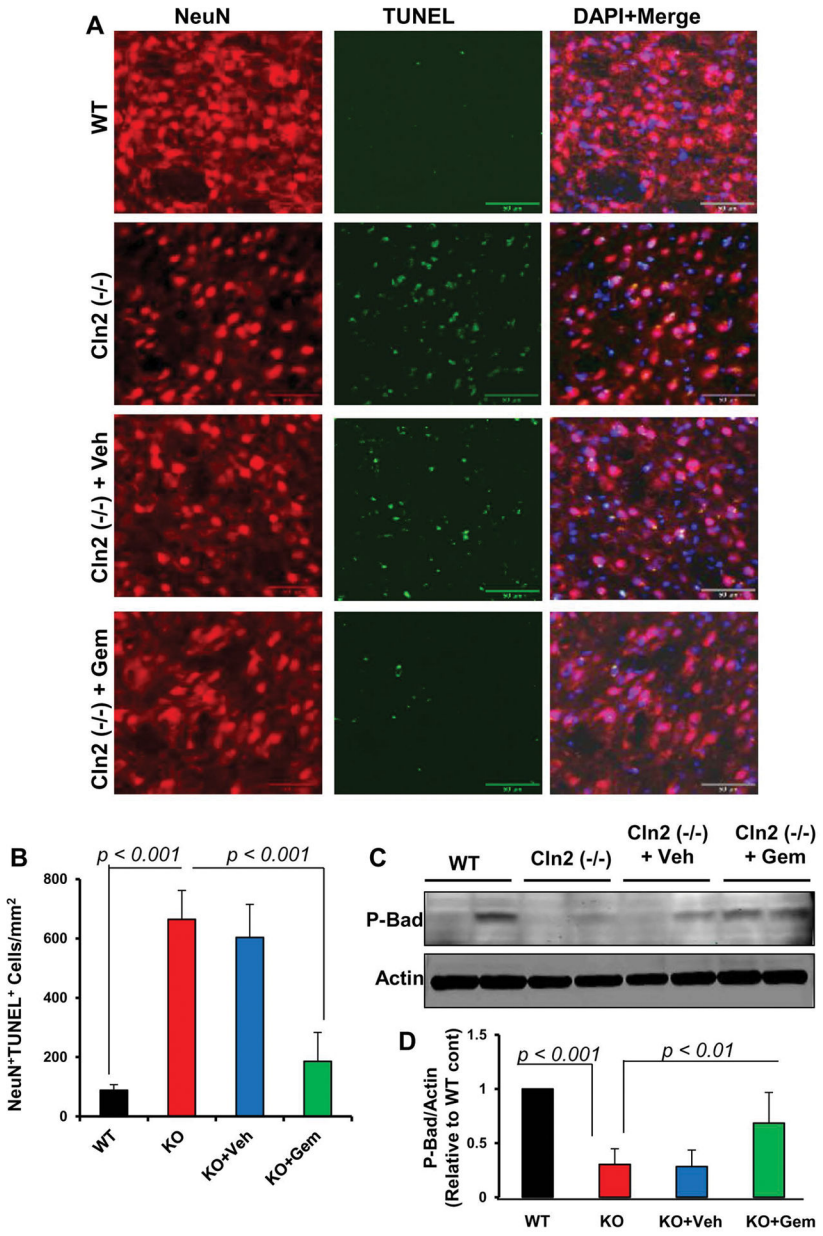


**Figure 5. Gem treatment inhibits apoptosis *in vivo* in the striatum of *Cln2* $^{(-/-)}$ mice**

*Cln2* $^{(-/-)}$ animals (4 weeks old) were treated with gem (dissolved in 0.1% MeC) orally at a dose of 7.5 mg/kg body weight/day. After 8 weeks of treatment, striatal sections were double-labeled for NeuN and TUNEL (A). $NeuN^{+}TUNEL^{+}$ cells were counted (B) in two different sections of each of six different mice (n=6) per group in an Olympus IX81 fluorescence microscope using the MicroSuite imaging software. C) Striatal homogenates were immunoblotted for phospho-BAD. Actin was run as loading control. D) Bands were scanned and values (P-BAD/Actin) are presented as relative to WT control. Results are mean ± SEM of four mice per group.

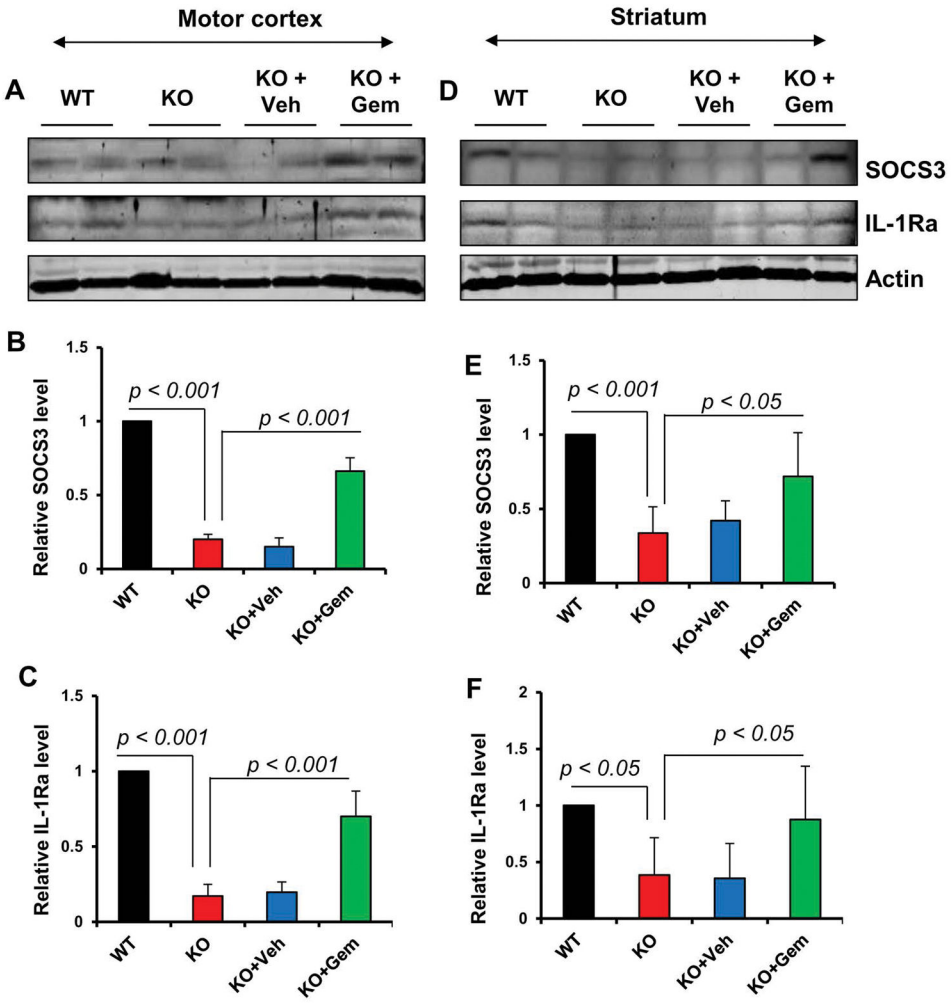


**Figure 6. Gem treatment upregulates the expression of anti-inflammatory molecules *in vivo* in the CNS of *Cln2* $^{(-/-)}$ mice**

*Cln2* $^{(-/-)}$ animals (4 weeks old) were treated with gem (dissolved in 0.1% MeC) orally at a dose of 7.5 mg/kg body weight/day. After 8 weeks of treatment, the expression of SOCS3 and IL-1Ra was monitored in motor cortex (A–C) and striatum (D–F) extracts by Western blot. Actin was run as loading control. Bands were scanned and values (SOCS3/Actin, B & E; IL-1Ra/Actin, C & F) are presented as relative to WT control for cortex (B & C) and striatum (E & F). Results are mean ± SEM of four mice per group.

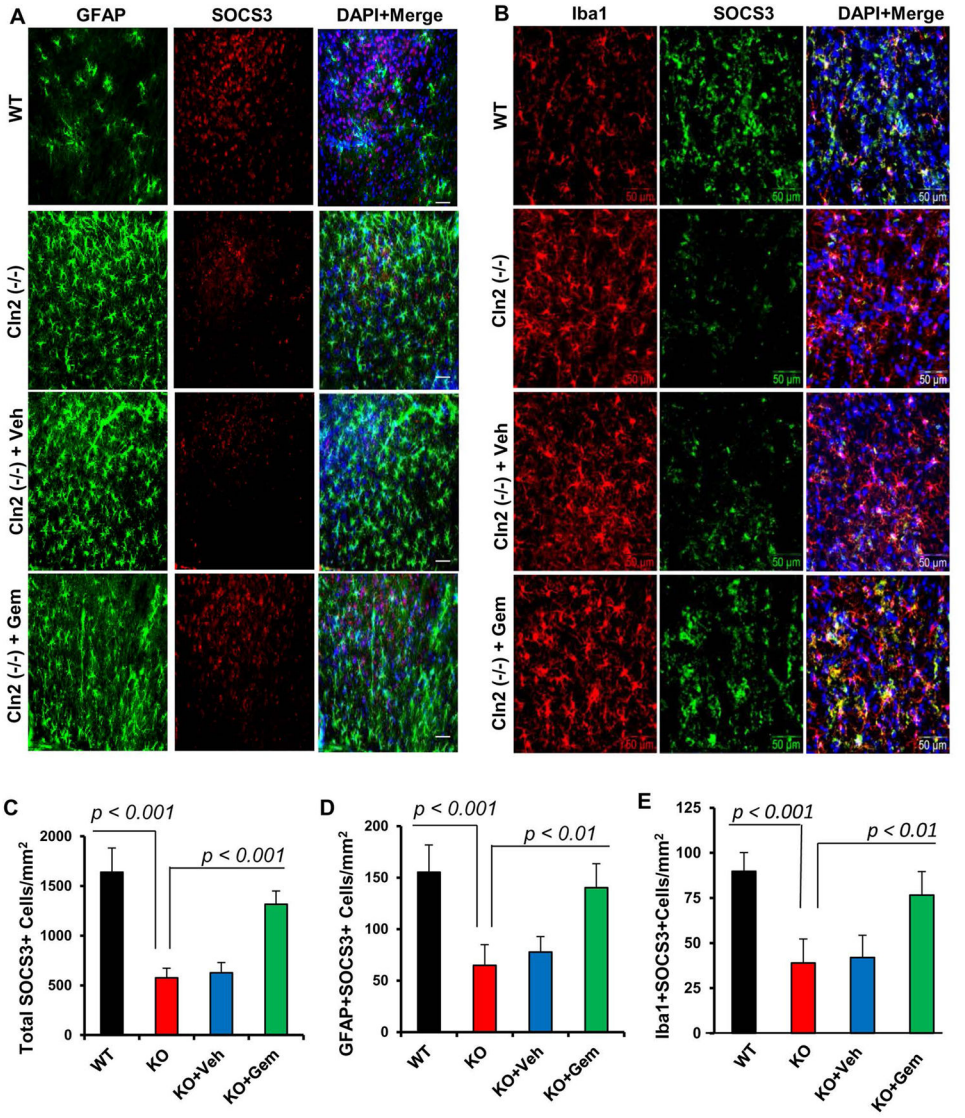


**Figure 7. Gem treatment upregulates SOCS3 *in vivo* in the striatum of *Cln2* $^{(-/-)}$ mice**

*Cln2* $^{(-/-)}$ animals (4 weeks old) were treated with gem (dissolved in 0.1% MeC) orally at a dose of 7.5 mg/kg body weight/day. After 8 weeks of treatment, striatal sections were double-labeled for GFAP & SOCS3 (A) and Iba1 & SOCS3 (B). Total SOCS3$^{+}$ (C), GFAP$^{+}$SOCS3$^{+}$ (D) and Iba1$^{+}$SOCS3$^{+}$ (E) cells were counted in two different sections of six different mice per group in an Olympus IX81 fluorescence microscope using the MicroSuite imaging software. Results are mean ± SEM of six mice per group.

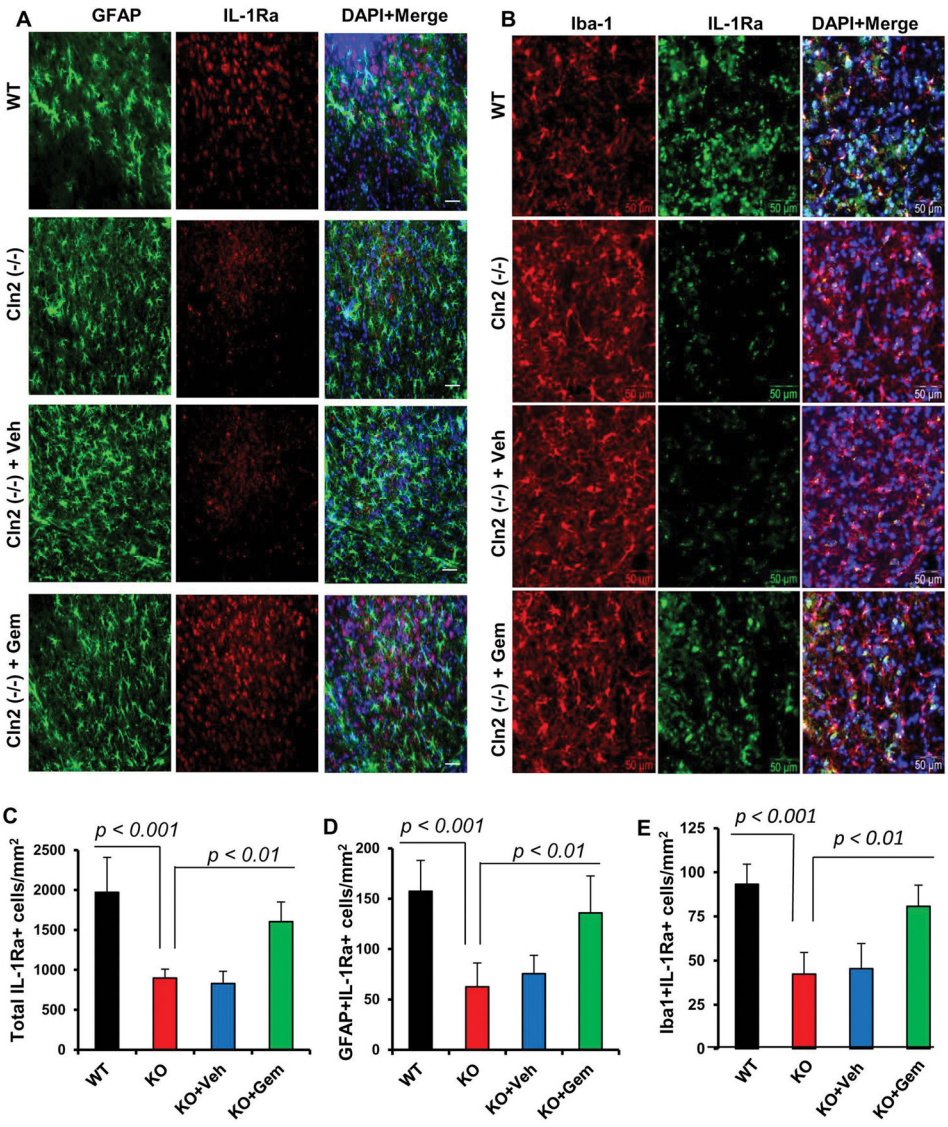


**Figure 8. Gem treatment upregulates IL-1Ra *in vivo* in the striatum of *Cln2* $^{(-/-)}$ mice**

*Cln2* $^{(-/-)}$ animals (4 weeks old) were treated with gem (dissolved in 0.1% MeC) orally at a dose of 7.5 mg/kg body weight/day. After 8 weeks of treatment, striatal sections were double-labeled for GFAP & IL-1Ra (A) and Iba1 & IL-1Ra (B). Total IL-1Ra$^{+}$ (C), GFAP$^{+}$IL-1Ra$^{+}$ (D) and Iba1$^{+}$IL-1Ra$^{+}$ (E) cells were counted in two different sections of six different mice per group in an Olympus IX81 fluorescence microscope using the MicroSuite imaging software. Results are mean ± SEM of six mice per group.

## Table 1

Antibodies, sources, applications, and dilutions used in this paper

| Target | Antibody (Clone) | Epitope/Immunogen | Application/Dilution | Source; Catalog |
|---|---|---|---|---|
| β-Actin | Mouse monoclonal (AC-15) | a.a. 1–15 of *Xenopus laevis* β-actin | WB – 1:5000 | Abcam; ab6276 |
| Subunit C of ATP synthase | Rabbit monoclonal | Synth peptide a.a. 50-C terminus Human ATP synthase | IHC – 1:100 | Abcam; ab181243 |
| GFAP | Rabbit polyclonal | Synth peptide to cow GFAP | IHC – 1:2000 | Dako; z0334 |
| Iba1 | Goat polyclonal | Synth peptide a.a. 135–147 Human Iba1 (C terminus) | IHC – 1:500 | Abcam; ab5076 |
| NeuN | Mouse monoclonal (A60) | Purified mouse brain nuclei | IHC – 1:500 | Millipore; MAB377 |
| P-BAD | Rabbit polyclonal | P-BAD (Ser 136) | WB – 1:300 | Cell Signaling; # 9295 |
| SOCS3 | Rabbit polyclonal | C-terminus of human SOCS3 | WB – 1:500 IHC – 1:200 | Abcam; ab16030 |
| IL-1Ra | Rabbit monoclonal | Human IL-1RA aa 150 to the C-terminus | WB – 1:500 IHC – 1:200 | Abcam; ab124962 |

WB, Western blot; IHC, immunohistochemistry; GFAP, glial fibrillary acidic protein; SOCS3, suppressor of cytokine signaling 3; IL-1Ra, Interleukin-1 receptor antagonist